Interferometric detection of a single vortex in a dilute Bose-Einstein condensate

F. Chevy, K. W. Madison, V. Bretin, and J. Dalibard

Laboratoire Kastler Brossel,* Département de Physique de l'Ecole Normale Supérieure, 24 rue Lhomond, 75005 Paris, France

Using two radio frequency pulses separated in time we perform an amplitude division interference experiment on a rubidium Bose-Einstein condensate. The presence of a quantized vortex, which is nucleated by stirring the condensate with a laser beam, is revealed by a dislocation in the fringe pattern.

The experimental realization of Bose-Einstein condensation of dilute atomic gases has opened for study a whole new class of macroscopic quantum systems [1]. In particular, the question of the superfluidity of a dilute condensate can now be addressed experimentally by analyzing the response of such a system to a moving perturbation. This response is severely restricted by the strong constraints that exist on the velocity field of the condensate. For a macroscopic wave function $\psi(\mathbf{r}) = \sqrt{n(\mathbf{r})}e^{iS(\mathbf{r})}$, where $n(\mathbf{r})$ is the density of the condensate and $S(\mathbf{r})$ the local phase, the velocity field is $(\hbar/M)\nabla S$, where M is the mass of a particle of the fluid. This relation requires that the circulation of the velocity field around any closed contour be quantized and equal to $\kappa h/M$, where κ is an integer [2,3]. A nonzero value of κ is associated with the presence of one or several quantum vortices. Such a vortex is characterized by a line along which the condensate density vanishes and around which the phase of the wave function varies by $2\kappa\pi$ (for recent reviews, see [4,5]).

A reliable way to nucleate a quantum vortex in a dilute Bose-Einstein condensate is to place the system in a rotating potential as was originally done with superfluid helium in the famous "rotating bucket experiment" [6,7]. Starting with a condensate confined in a cylindrically symmetric trap, one can stir the atomic cloud using an additional rotating anisotropic potential created by the dipole potential of a nonresonant stirring laser beam [8,9]. There exists a range of values of the stirring frequency for which one can nucleate in this way a single vortex that will center itself on the symmetry axis of the trap. The presence of the vortex is then revealed by the existence of a density dip at the center of the spatial distribution of the condensate. Further experiments have also revealed that the angular momentum per particle is equal to $\hbar$ for this centered, one-vortex state [10,11].

We present in this Rapid Communication a direct observation of the phase of such a rotating condensate. We follow the scheme proposed in [12–15], which relies on an interferometric measurement. Here, we divide the wave function of the condensate into two components separated in position and momentum. In the location where these components overlap, a matter-wave interference fringe pattern is produced that reveals the phase difference between the two

components. This homodyne detection of the phase pattern of the vortex state of the condensate is analogous to the experiments aiming at studying the transverse phase structure of optical Laguerre-Gauss modes [16]. Moreover, it is complementary to the heterodyne detection of a vortex state performed in Boulder in 1999 [17]. In that experiment, a vortex was created in a two component condensate by a direct printing of the vortex state phase $e^{i\theta}$ on one of the two components (θ is the azimuthal angle around the symmetry axis of the condensate). The second component, corresponding to a different internal state of the atoms, remained at rest at the center of the confining potential and was used as a "reference" matter wave to detect the phase of the vortex state contained in the rotating component. In this case, the two interfering components correspond to two amplitudes with a different spatial phase, while in our case the two components have the same spatial phase but are shifted in position and momentum.

We prepare our Bose-Einstein condensate by evaporative cooling of 10^8 rubidium (^{87}Rb) atoms confined in a Ioffe-Pritchard trap. The trap is axisymmetric and its eigenfrequencies are respectively $\omega_\perp = 2\pi \times 192$ Hz and $\omega_z = 2\pi \times 11.7$ Hz for the stretched state $m = +2$ of the $5S_{1/2}$,F $= 2$ ground state. The initial temperature of the atom cloud, which is precooled using optical molasses, is 100 μK. At the end of the evaporation, a condensate containing 3×10^5 atoms is formed, and the temperature of the cloud is below 100 nK. We then nucleate the vortices by the method described in [8]: we superimpose to the isotropic magnetic trap a far detuned laser beam propagating along the weak horizontal axis (z) of the trap and positioned by two crossed acousto-optic modulators. This light beam creates in the xy plane an anisotropic optical dipole potential of the form $\delta U(X,Y) = \epsilon M \omega_\perp^2 (X^2 - Y^2)/2$. We rotate at constant frequency $\Omega/2\pi \sim 130$ Hz the eigenaxes XY of this potential, which provides the desired stirring, with $\epsilon = 0.06$ in the present experiment. We stir the atomic cloud for a duration of 300 ms. We verified in a preliminary step that this duration is sufficiently long to nucleate a well centered single vortex.

To realize the amplitude splitting interferometer, we use a method similar to the one described in [18]. A succession of two rf pulses, which resonantly drive transitions between different internal states of each rubidium atom, is used to coherently split and recombine the condensate cloud. The atomic rubidium condensate is initially polarized the $F = m = 2$ Zeeman substate. The first rf pulse couples this magnetic
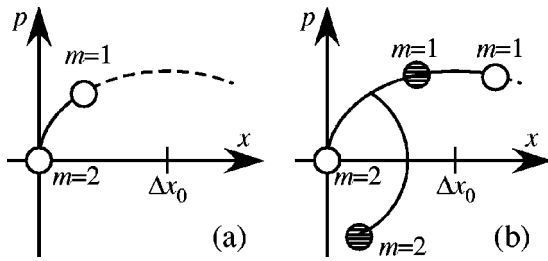
_____

FIG. 1. Phase-space trajectories of the $m=+2/m=+1$ Zeeman substate wave packets in the harmonic trapping potential during the experimental sequence. (a) location of the two wave packets at a time τ_1 after the first rf pulse. (b) location of the four confined wave packets at a time τ_2 after the second rf pulse. The hatched disks correspond to the wave packets generated by the second rf pulse.

spin state to the four other Zeeman substates of the $F=2$ manifold. Among these four, only the $m=+1$ is also magnetically trapped. However, due to gravity, the center of its confining potential is vertically displaced with respect to the center of the $m=+2$ trap by an amount $\Delta x_0 = g/\omega_{\perp}^2 \approx 6$ μm. After this first pulse, the atoms are allowed to evolve in the harmonic trapping potential for a variable time τ_1. During this time, those atoms driven into the other Zeeman substates fall or are ejected out of the trap. What remains are the two trapped clouds now with slightly different momenta and positions as determined by their respective phase space trajectories pictured in Fig. 1(a). When the second rf pulse is applied, each trapped state generates a copy in the other trapped Zeeman sublevel making a total of four wave packets present in the trap (two in $m=+1$ and two in $m=+2$). We then let the atoms evolve in the harmonic potential for a time τ_2 [Fig. 1(b)] after which we extinguish the trapping potential and let the condensate clouds freely expand and fall for 25 ms. Finally, we record the atomic interference pattern between the overlaping wave packets of a given internal Zeeman spin state using the resonant absorption imaging technique originally used to detect the density dip associated with the vortex line.

The possibility of changing independently τ_1 and τ_2 allows for an independent control of the initial relative velocity and separation of two interfering wave packets. Note that the amplitude of these rf pulses is large enough so as to resonantly excite all atoms in the condensate, in spite of the inhomogeneity of the magnetic field inside the trap. This requires that the Rabi frequency Ω_{rf} associated with these rf excitations be at least of the order of $\mu/\hbar$, where μ is the chemical potential. In our case, $\mu/\hbar$ is typically $2\pi \times 10$ kHz, while $\Omega_{rf}=2\pi \times 7$ kHz. The duration of each rf pulse is 13 μs which ensures that the populations of the two states $m=+2$ and $m=+1$ after each pulse are comparable.

Before showing the interference patterns detected experimentally, we present a simple theoretical model to discuss the type of signal that can be expected. Consider first a trapped condensate localized around $\mathbf{r}=0$ with no velocity field ($\psi(\mathbf{r})=\sqrt{n(\mathbf{r})}$). We assume that this condensate is split into two parts separated by $\mathbf{a}$, so that the unnormalized state of the system is $\psi(\mathbf{r}-\mathbf{a}/2)+\psi(\mathbf{r}+\mathbf{a}/2)$. The potential confining the atoms is then extinguished and the two clouds
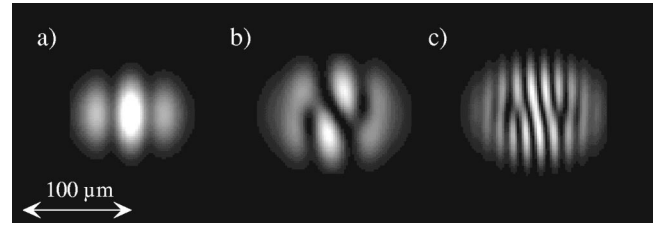

FIG. 2. Expected fringe pattern of a Bose-Einstein condensate initially splitted into two parts and undergoing a free expansion phase. Figure (a) is without a vortex and (b,c) are with a vortex. For (b), close to our experimental conditions, the fringe spacing x_s is equal to 39 μm, and it is equal to the separation of the vortex cores after expansion $|\mathbf{r}_1-\mathbf{r}_1'|$. (c) same as (b), with a fringe spacing $x_s = 13$ μm$=|\mathbf{r}_1-\mathbf{r}_1'|/3$ (this fringe spacing is too small to be detected in our experimental setup). For (b) and (c), the relative phase of the two condensates is π.

overlap and interfere. The detection of the interference pattern is done at a time t large enough so that the final size of the condensate is much larger than the initial one. Consequently a model relying on a noninteracting Bose-Einstein condensate is sufficient to interpret the fringe pattern [19–21]. The phase pattern of the wave function issued from the condensate initially localized in $\mathbf{r}_0=\pm\mathbf{a}/2$ is the same as that of the function

$$\Phi(\mathbf{r}) = \exp\left(\frac{iM(\mathbf{r}-\mathbf{r}_0)^2}{2\hbar t}\right), \tag{1}$$

so that the interference pattern consists in parallel fringes, with a fringe spacing [22]

$$x_s = \frac{ht}{Ma}. \tag{2}$$

The phase pattern of Eq. (1) remains valid even if the cloud initially localized in $\mathbf{r}_0$ has a nonzero mean velocity. Therefore the expression for the fringe spacing (2) is still correct when the relative velocity of the two interfering clouds is not zero, provided a denotes the *initial* spatial separation between the centers of the condensates before the atoms were released [18]. Note that the size of the expanding condensates also increases linearly with t, so that the number of visible fringes is independent of the expansion time. In practice, the number of visible fringes is limited by the optical resolution δx of the imaging system ($\delta x=7$ μm in our experiment), since one must have $\delta x \ll x_s$. Choosing the maximal value of the expansion time compatible with our experimental setup (25 ms) gives from Eq. (2) the product $x_s a \sim (11$ μm$)^2$. Then for a good fringe visibility, we choose a small value of a, typically $a=2.5$ μm, which yields $x_s \sim 45$ μm. The diameter of the condensate after expansion is 100 μm, so that three bright fringes should be clearly visible in the interference pattern. The corresponding calculated pattern is shown in Fig. 2(a) assuming an initial Gaussian distribution with an r.m.s. width $\Delta x = \Delta y = 0.5$ μm, a separation $a=2.9$ μm and an expansion time of 25 ms, yielding $x_s=39$ μm.

Consider now a condensate centered at $\mathbf{r}=\mathbf{r}_0$, and assume that a quantized vortex, with an angular momentum $+\hbar$ with respect to the z axis, sits at the center of the condensate. The initial wave function of the condensate is $\psi(\mathbf{r})=(x-x_0+i(y-y_0))f(|\vec{\rho}-\vec{\rho}_0|,z)e^{i\mathbf{k}\cdot\mathbf{r}}$. Here we use cylindrical coordinates $(\vec{\rho},z)$ with respect to the z axis, and f is a function of $|\vec{\rho}|$ and z with a constant phase. When the condensate is released from the trap and expands for a time t, the phase pattern of the cloud wave function is equal to that of the function Φ' defined as

$$\Phi'(\mathbf{r})=(x-x_1+i(y-y_1))\exp\left(\frac{iM(\mathbf{r}-\mathbf{r}_0)^2}{2\hbar t}\right), \qquad (3)$$

where we set $\mathbf{r}_1=\mathbf{r}_0+\mathbf{v}_0 t$. Note that we allow for a possible nonzero velocity $\mathbf{v}_0=\hbar\mathbf{k}/M$ of the center of mass of the condensate. This result can be shown first for a cloud initially at rest ($\mathbf{v}_0=0$), and can then be generalized to a moving cloud using a Galilean transform.

The expected signal in an interference experiment can be obtained by superposing two wavefunctions varying as (3), obtained by expanding two condensates initially located at $\mathbf{r}_0=\mathbf{a}/2$ and $\mathbf{r}_0'=-\mathbf{a}/2$, with initial velocities $\mathbf{v}_0$ and $\mathbf{v}_0'$. The interference pattern consists in parallel lines separated by $x_s=ht/Ma$, with "defects" associated with the presence of the vortex. These defects are clearly visible if the distance $\mathbf{r}_1-\mathbf{r}_1'=\mathbf{a}+(\mathbf{v}_0-\mathbf{v}_0')t$ between the two vortex cores after expansion is larger than x_s. Since a is very small compared to x_s in our setup, this visibility condition requires that

$$\Delta v \geqslant \frac{h}{Ma}, \qquad (4)$$

where $\Delta v=|\mathbf{v}_0-\mathbf{v}_0'|$. On the other hand Δv should be smaller than the velocity width of each condensate after expansion, so that the two clouds overlap after the time of flight. In practice, we choose the times τ_1 and τ_2 so that Eq. (4) is close to being an equality and the overlap of the two wave packets after expansion is maximized. The centers of the two vortices after expansion are then separated by the fringe spacing x_s and one expects the characteristic fringe pattern shown in Fig. 2(b), with two dislocations ("H" shape) indicating the centers of the two vortices after time of flight. In Fig. 2(c), we show the fringe pattern that would be expected for a larger initial separation a, where more fringes are visible.

We now turn to the discussion of the experimental results. We have first measured the interference pattern in the absence of any vortices. As expected, this pattern consists in straight fringes, and a typical result is shown on Fig. 3. The two patterns corresponding to the $m=+2$ and $m=+1$ components are recorded simultaneously. The spatial separation between these two components results from the difference between the initial velocities of the $m=+1$ and $m=+2$ clouds when released from the trap. The difference in the fringe spacings reflects the fact that the initial separation a_1 between the two wave packets in state $m=+1$ was larger than the separation a_2 between the two wave packets in m
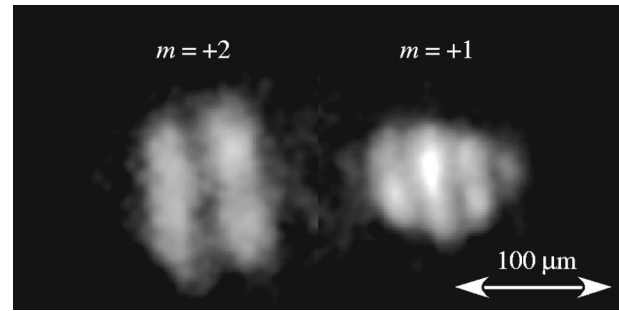

FIG. 3. Interference pattern of a nonrotating condensate split into four parts (two in each Zeeman state $m=+2$ and $m=1$), which overlap during the free expansion phase. Here $\tau_1=0.3$ ms and $\tau_2=0.4$ ms.

$=+2$ (see e.g. Fig. 1). We have checked for each component that the variation of the fringe spacing with $a_{1,2}$ is in good agreement with Eq. (2) (see also [18]). In the following we use the interference pattern obtained with the $m=2$ component, which offers a better visibility due to its larger spatial extent after time of flight, which is itself due to a stronger confinement in the trap.

When we stir the atomic cloud at a frequency of 130 Hz (close to the critical frequency $\omega_\perp/\sqrt{2}$ [23]), a well centered, single vortex is created in the condensate. The result from an interference experiment performed in this case is shown on Fig. 4(b) for the $m=+2$ channel. This pattern, which is very different from the one obtained with a slightly slower rotation (125 Hz) at which no vortex nucleation occurs [Fig. 4(a)], is the main result of this paper. It clearly shows the telltale "H" shape characteristic of the 2π phase winding due to the presence of a vortex [see Fig. 2(b)]. We repeated
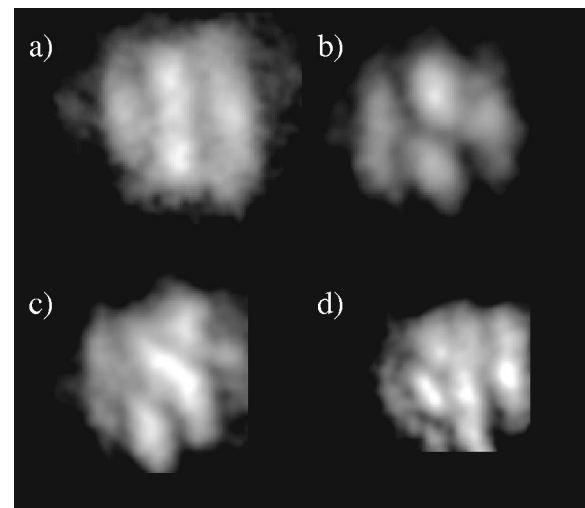

FIG. 4. Interference pattern measured in the $m=+2$ channel with no (a), one (b) and (c), and several (d) vortices. For these pictures, $\tau_1=0.688$ ms and $\tau_2=1.320$ ms. The stirring frequency was set to $\Omega=2\pi\times125$ Hz (a), $\Omega=2\pi\times130$ Hz (b-c), and $\Omega=2\pi\times154$ Hz (d). The patterns (b) and (c) were recorded with the same initial conditions, and the change in the interference pattern results from a change in the relative phase of the two parts of the condensate.

this experiment many times for the same initial condition, and have found that the interference patterns produced have a similar shape, but with a relative phase between the two components that fluctuates from one shot to another so that the bright and dark regions in Fig. 4(b) can be exchanged [see e.g., Fig. 4(c)]. Finally, when several vortices are nucleated by stirring at a higher frequency, the fringe structure is more complex and the number of fringe dislocations is larger [Fig. 4(d)].

In conclusion, we have observed the 2π-phase shift associated with the presence of a vortex in a single component Bose-Einstein condensate by using an interferometric detection method. This technique can be used as a very sensitive tool to diagnose the presence of vortices generated by the fast motion of a macroscopic object in a condensate. This was demonstrated very recently at Massachusetts Institute of Technology, in an experiment where the interference pattern between a condensate with vortices and a condensate at rest has been recorded [24].

The ''beam splitter'' used here is very simple, since it consists of a resonant radio frequency pulse. However, one disadvantage of this type of beam splitter is the unavoidable loss of atoms to the other untrapped Zeeman states resulting in at most only $\sim 1/3$ of the atoms participating in the interference signal in the $m = +2$ channel. We plan to use in the near future a more efficient scheme discussed in [15], which involves the use of two Bragg pulses to couple just two states of different momentum.

[1] For a review, see e.g., *Bose-Einstein Condensation in Atomic Gases*, Proceedings of the International School of Physics ''Enrico Fermi,'' edited by M. Inguscio, S. Stringari, and C. Wieman (IOS Press, Amsterdam, 1999).

[2] L. Onsager, Nuovo Cimento **6**, 249 (1949).

[3] R.P. Feynman, in *Progress in Low Temperature Physics*, edited by C.J. Gorter (North-Holland, Amsterdam, 1955), Vol. 1.

[4] F. Dalfovo *et al.*, Rev. Mod. Phys. **71**, 463 (1999).

[5] A. Svidzinsky and A. Fetter, J. Phys.: Condens. Matter **13**, R135 (2001).

[6] E.M. Lifshitz and L.P. Pitaevskii, *Statistical Physics, Part 2*, Chap. III (Butterworth-Heinemann, 1980).

[7] R.J. Donnelly, *Quantized Vortices in Helium II* (Cambridge University Press, Cambridge, 1991).

[8] K.W. Madison *et al.*, Phys. Rev. Lett. **84**, 806 (2000).

[9] J.R. Abo-Shaeer *et al.*, Science **292**, 467 (2001).

[10] F. Chevy, K. Madison, and J. Dalibard, Phys. Rev. Lett. **85**, 2223 (2000).

[11] P.C. Haljan *et al.*, Phys. Rev. Lett. **86**, 2922 (2001).

[12] E.L. Bolda and D.F. Walls, Phys. Rev. Lett. **81**, 5477 (1998).

[13] J. Tempere and J.T. Devreese, Solid State Commun. **108**, 993 (1998).

[14] Y. Castin and R. Dum, Eur. Phys. J. D **7**, 399 (1999).

[15] L. Dobrek *et al.*, Phys. Rev. A **60**, R3381 (1999).

[16] I.V. Basistiy *et al.*, Opt. Commun. **103**, 422 (1993).

[17] M.R. Matthews *et al.*, Phys. Rev. Lett. **83**, 2498 (1999).

[18] C. Fort *et al.*, e-print cond-mat/0101386.

[19] Y. Castin and R. Dum, Phys. Rev. Lett. **77**, 5315 (1996).

[20] Yu. Kagan, E.L. Surkov, and G.V. Shlyapnikov, Phys. Rev. A **55**, R18 (1997).

[21] More precisely, if the two parts of the condensate are initally well separated, the interaction between these parts is negligible, since the density is already very low when they start to overlap. The only effect of the mean-field interaction (within each part) is a modification of the envelope of the interference pattern.

[22] M.R. Andrews *et al.*, D.M. Kurn, and W. Ketterle, Science **275**, 637 (1997).

[23] K. Madison *et al.*, Phys. Rev. Lett. **86**, 4443 (2001).

[24] S. Inouye *et al.*, e-print cond-mat/0104444.